

# Nanoscale Heterogeneities in Nematic Azobenzene Polymethacrylates for Optical Nanowriting

Giancarlo Galli,<sup>\*1</sup> Istvan Szanka,<sup>1</sup> Laura Andreozzi,<sup>2</sup> Ciro Autiero,<sup>2</sup> Massimo Faetti,<sup>2</sup> Marco Giordano,<sup>2</sup> Fabio Zulli<sup>2</sup>

**Summary:** ESR studies of the rotational dynamics of the cholestane spin probe dissolved in nematic azobenzene polymethacrylates from above  $T_{NI}$  to below  $T_g$  are presented. Different dynamic regimes were recognized, in which the molecular sites or distributions of molecular sites were populated depending on the structure of the polymers and their thermal histories. We highlight the significance of such spatial-temporal nanoscale heterogeneities in view of possible application of the azobenzene polymers in erasable optical nanowriting.

**Keywords:** azobenzene; dynamics; electron spin resonance; liquid-crystalline polymer; nanowriting; optical storage

## Introduction

Azobenzene polymers are some of the most extensively studied photochromic materials in soft matter. They include various structures of liquid-crystalline (LC) polymers in which the azobenzene mesogen is typically located in the side chains as a pendant group. In addition to photochromism, azobenzene can undergo a readily induced and reversible photoisomerization between the *trans* and *cis* isomers.<sup>[1]</sup> This interconversion effects control over a variety of chemical, mechanical, electronic, and optical properties.<sup>[2]</sup> Azobenzene polymers have in fact been used in the areas of holography, optical data storage, integrated optics, molecular switches, and all-optical modulation.

In our studies of the erasable optical storage in azobenzene nematic polymers,<sup>[3,4]</sup> we could imprint 50 nm and 120 nm information bits by topography and birefringence patterning, respectively, the resolution being limited in any case by

the optics of the near-field scanning optical microscope used for the inscription. An estimate of the ultimate size of the optically imprinted bit is seemingly in the range of the cooperativity and entanglement lengths, 3–10 nm, which would correspond to a storage density as high as  $\sim 1$  Tbyte/cm<sup>2</sup>. However, heterogeneity at the molecular level may substantially affect the bit stability, thus seriously limiting the effectiveness of the azobenzene polymers as optical storage materials at the nanometer length scale.

For fundamental understanding of the reorientation processes and their correlation with the local environment in side group polymers, electron spin resonance (ESR) can play a major role due to its well known sensitivity to time (ns) and length (nm) scales.<sup>[5]</sup> ESR spectroscopy studies of spin probe guests dissolved in polymeric hosts have appeared in literature,<sup>[6–9]</sup> even though an accurate evaluation of the spin dynamics in heterogeneous systems has seldom been performed.<sup>[5,10,11]</sup> The nature of the spin probe dynamics, depending on both molecular geometry and the peculiar features of the host matrix, affects significantly the ESR line shape. Heterogeneity in the probe dynamics is observed when its lifetime becomes larger than the measuring

<sup>1</sup> Dipartimento di Chimica e Chimica Industriale, Università di Pisa e Consorzio INSTM, 56126 Pisa, Italy  
E-mail: gallig@ccci.unipi.it

<sup>2</sup> Dipartimento di Fisica 'E. Fermi', Università di Pisa, polyLab-CNR, 56127 Pisa, Italy

observation time, i.e. the spin-spin relaxation time. Space heterogeneity manifests itself with a distribution of sites available to the host molecule, which in turn determines a distribution of correlation times  $\tau$ . For example, in azobenzene polymethacrylates the molecular sites available to rotation of the cholestane spin probe exhibited a discrete distribution of  $\tau$  depending on the thermal treatment.<sup>[4,12]</sup>

In this work we studied the ESR dynamics of the cholestane spin probe in a series of azobenzene polymethacrylate hosts, denoted as PMA4, in which the molar mass and its dispersity were varied in the homopolymer samples, as well as the chemical composition in the copolymer samples (Figure 1). We found different spatial-temporal nanoscale heterogeneities in such polymers and highlight their significance in the perspective of application of the azobenzene polymers in reversible optical nanowriting.

## Experimental Part

General procedures can be found in the literature for the synthesis of the polymers (AIBN polymerization)<sup>[13]</sup> and the oligomer (BriBuCOOMe/HMTETA/CuBr polymerization).<sup>[14]</sup>

Rheological measurements in the oscillatory regime were carried out with a Haake Rheostress RS150H rheometer in the plate-cone geometry at temperatures ranging from  $T_g$  up to  $T_g + 120$  K. The temperature dependence of the shear viscosity  $\eta$  in the investigated regions was

well described by the Vogel-Fulcher (VF) law (Eq. 1). The relevant pseudo-activation energy ( $T_b$ ) and Vogel temperature ( $T_0$ ) are collected in Table 1.

$$\eta(T) = \eta_{\infty} \exp\left(\frac{T_b}{T - T_0}\right) \quad (1)$$

ESR studies were performed on the polymeric matrices in which the cholestane spin probe was dissolved ( $10^{-3}$  cholestane/repeat unit mole ratio). Reproducible results of the probe dynamics were obtained by annealing the samples at  $T_a$  according to a special protocol.<sup>[5,16]</sup> An X band Bruker ER 200 SRL was used and the temperature control ( $\pm 0.1$  K accuracy) was ensured by a Bruker BVT100 system. ESR spectra were simulated by using a theoretical approach based on generalized Mori theory.<sup>[17]</sup> The cholestane spin probe exhibits nearly axial symmetry.<sup>[18]</sup> Its reorientational dynamics in the polymer matrices was characterized by a spinning motion around its own symmetry axis and a tumbling motion of the symmetry axis itself with correlation times  $\tau_{||}$  and  $\tau_{\perp}$ , respectively. The anisotropy ratio  $\tau_{\perp}/\tau_{||}$  was found to be 15 for the oligomer, homopolymer, and 40/60 copolymer, and 18 for the 30/70 copolymer over the whole temperature range. Therefore, only the temperature dependence of  $\tau_{||}$  will be shown. The greater  $\tau_{\perp}/\tau_{||}$  presented by the 30/70 copolymer denotes that the molecular tracer reoriented in a more rigid molecular environment. The principal components of the magnetic tensors of the spin probe were drawn by the powder line shapes of the linear ESR recorded at 143 K, according to the procedure described elsewhere.<sup>[19]</sup>

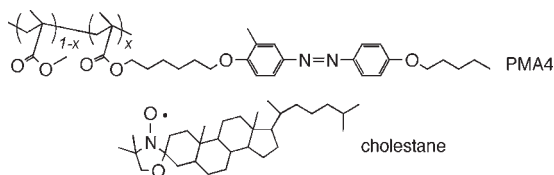


**Figure 1.**

Structures of the PMA4 homopolymer ( $x=1$ ) and copolymer ( $x=0.7$  and  $0.6$ ) hosts and the cholestane spin probe guest.

**Table 1.**VF fit parameters for the PMA4 samples.<sup>a)</sup>

PMA4 sample	$\eta_{\infty}$ (Pa s)	$T_b$ (K)	$T_o$ (K)
Oligomer		1150 $\pm$ 150	244
Homopolymer	$(2.12 \pm 0.03) \cdot 10^{-3}$	1300 $\pm$ 30	259 $\pm$ 5
40/60 Copolymer	$(7.5 \pm 0.3) \cdot 10^{-3}$	1960 $\pm$ 70	258 $\pm$ 2
30/70 Copolymer	$(2.0 \pm 0.2) \cdot 10^{-3}$	1570 $\pm$ 50	266 $\pm$ 2

<sup>a)</sup> Data for the oligomer were evaluated in [15].

The values of the Zeeman and hyperfine tensors in the molecular frame are listed in Table 2.

## Results and Discussion

Several PMA4 samples were investigated, including an oligomer and a homopolymer of very different molar masses and molar mass distributions, and copolymers with methyl methacrylate of different chemical compositions. The oligomer was prepared by the atom transfer radical polymerization (ATRP) technique, while the other samples were prepared by classic free radical polymerization. The former method allows for better control over  $M_w$  and  $M_w/M_n$  of the polymers (Table 3). With the exception of the not LC 40/60 copolymer, the PMA4 samples formed a nematic phase between  $T_g$  and  $T_{NI}$  (Table 3). The homopolymer also underwent a conformational transition at  $T_{conf}$ , which is ascribed to the increased nematic potential when temperature is lowered to  $T_g$ .<sup>[4]</sup>

Linear ESR investigations<sup>[5,20]</sup> performed on different spin probes in molecular and polymeric glass formers have shown that the reorientational correlation times of paramagnetic probe follow frac-

tional laws  $(\eta/T)^{\xi}$ ,  $\eta$  being the viscosity of the host matrix. The fractional coefficient  $\xi$  accounts for the decoupling degree of the probe dynamics from the structural relaxation of the polymer main chain. It may be a manifestation of either steric hindrance or cooperativity effects in the dynamics of the polymer main chain.<sup>[5]</sup>

Many efforts were made to carefully take into account the heterogeneous nature of the ESR experimental line shapes of the PMA4 polymers.<sup>[9]</sup> The analysis led us to recognize the bimodal character of the distribution function of the spin probe sites. In fact, a two- $\delta$  distribution function of the correlation times with fast and slow reorienting sites was shown to reproduce the experimental line shape better than log-Gauss and square distributions. On the other hand, the simulations proved the homogeneous character of the ESR line shapes for the cholestane probe in the PMA4 oligomer, as one single value of  $\tau_{||}$  necessary to reproduce the experimental ESR line shapes for this sample (Figure 2).

Four regions (I–IV) were identified for the temperature dependence of  $\tau_{||}$  in the PMA4 oligomer (Figure 2a). Arrhenius trends with activation energies  $\Delta E_a$  were followed in the extreme temperature regions. For the two intermediate regions

**Table 2.**

Values of the principal components of the Zeeman and hyperfine tensors in the molecular reference frame for cholestane.

PMA4 sample	$g$			$A$ (G)		
	$g_{xx}$	$g_{yy}$	$g_{zz}$	$A_{xx}$	$A_{yy}$	$A_{zz}$
Oligomer	2.0025	2.0088	2.0062	33.0	6.5	5.5
Homopolymer and Copolymers	2.0026	2.0092	2.0069	32.6	5.5	5.0

**Table 3.**Physico-chemical characteristics of PMA4 samples.<sup>a)</sup>

PMA4 Sample	$M_w$ (g/mol)	$M_w/M_n$	$T_g$ (K)	$T_{conf}$ (K)	$T_{NI}$ (K)
Oligomer	7100	1.23	294		344
Homopolymer	59000	3.17	294	320	353
Copolymer 40/60	93200	4.01	320		
Copolymer 30/70	117000	3.54	314		345

<sup>a)</sup>  $T_g$ ,  $T_{conf}$ , and  $T_{NI}$  were measured according to the enthalpic, onset, and onset methods, respectively.

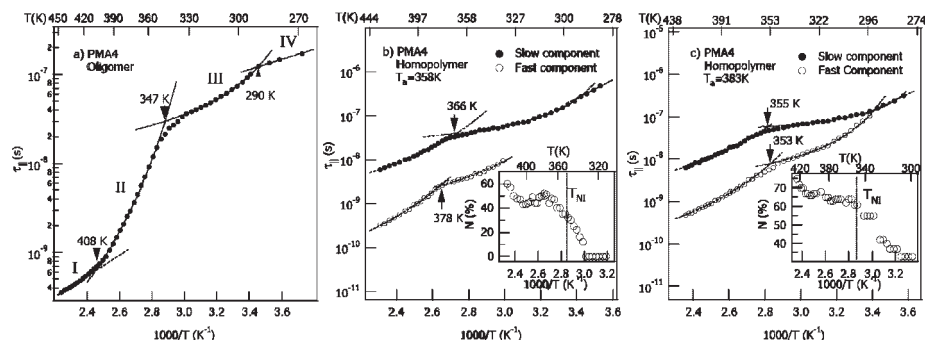
the temperature dependence was well described by the VF law (Eq. 2):

$$\tau_{||}(T) = \tau_{||\infty} \exp\left(\frac{T_b}{T - T_0}\right) \quad (2)$$

where  $\tau_{||\infty}$  and  $T_b$ , the pseudo-activation energy in K, are parameters dependent also on the spin probe, and  $T_0$  is the Vogel temperature. The values of the fit parameters are reported in Table 4. Note that  $T_b = 1070 \pm 50$  K for the high VF temperature region is the highest value found for the cholestane probe in all our studies in polymers. Owing to the substantial equality of the values of  $T_b$  of  $\tau_{||}$  and  $\eta$ , the fractional coefficient is  $\xi \approx 1$ , which points to the complete coupling of the probe dynamics to that of the polymer main chain. The crossover in the dynamics between the two VF regimes occurs at 347 K in correspondence of  $T_{NI}$ . The low value of  $T_b$  for the low temperature VF region indicates that the relevant molecular sites are likely situated away from the main

chain along the mesogenic side group near the terminal alkyl tails of the repeat unit. According to<sup>[5]</sup> the cooperativity coefficient  $\xi_c$  is given by the ratio between the  $T_b$  values of the intermediate region and the high temperature region; for the PMA4 oligomer we found  $\xi_c = 0.11$  that would correspond to  $1/\xi_c \approx 9$  cooperative repeat units.

It is interesting to compare the dynamics of the oligomer with that of the homopolymer after annealing at  $T_a = 383$  K and 358 K (Figures 2b, 2c). For the latter the fractional coefficient relevant to the probe dynamics at higher temperatures was traced to steric hindrance due to the specific local characteristic of the host matrix, while the one relevant to lower temperatures was ascribed to the onset of cooperativity in the dynamics.<sup>[5]</sup> Moreover, the analysis of the decoupling degree of probe dynamics from the structural relaxation allowed to characterize different molecular sites in which the spin probe reorients.<sup>[12]</sup> The best-fit VF

**Figure 2.**

Temperature dependence of ESR correlation times in the PMA4 oligomer (a) and homopolymer for the annealing procedures at  $T_a = 358$  K (b) and  $T_a = 383$  K (c). The insets show the population ( $N$ ) of the fast component.

**Table 4.**

Fit parameters for the temperature dependence of the cholestane spinning correlation time in the PMA4 oligomer in the different regimes.

Region	T range	Physical law	Fit parameters			
			$\tau_{  \infty}$	$\Delta E_a$	$T_o$	$T_b$
			(s)	(kJ/mol)	(K)	(K)
I	$T > 408$ K	Arrhenius	$(8.2 \pm 0.1) \cdot 10^{-13}$	$21 \pm 4$		
II	$347 \text{ K} < T < 408 \text{ K}$	Vogel-Fulcher	$(6.0 \pm 0.1) \cdot 10^{-13}$		$244 \pm 4$	$1070 \pm 50$
III	$290 \text{ K} < T < 347 \text{ K}$	Vogel-Fulcher	$(8.8 \pm 0.1) \cdot 10^{-9}$		$244 \pm 6$	$122 \pm 7$
IV	$T < 290$ K	Arrhenius	$(1.8 \pm 0.1) \cdot 10^{-9}$	$10 \pm 2$		

parameters for the fast and the slow sites in the two temperature regions are given in Table 5. The presence of different sites in the whole temperature range denotes the greatly heterogeneous character of the polymeric matrix annealed at 383 K (Figure 2c). By contrast, the fast component was unstable in the host matrix after annealing at 358 K and disappeared at about 328 K, that is very close to  $T_{\text{conf}}$  (Figure 2b). Thus, thermal annealing treatments slightly above  $T_{\text{NI}}$  are preferable in order to obtain a homogeneous matrix that should be suited for optical writing.

An Arrhenius law with  $\Delta E_a = (21 \pm 4)$  kJ/mol fits the activated regime in the highest temperature zone. An activated region at high temperature has already been found for unentangled polymer chains by ESR<sup>[9]</sup> and other techniques,<sup>[21]</sup> and is attributed to changes of the conformers along the main chain when they are able to rotate without restrictions by their nearest neighbors.<sup>[21]</sup> The comparatively high  $\Delta E_a$  of the PMA4 oligomer may be due to the

greater resistance opposed by the bulky azobenzene side group.

In contrast to the PMA4 homopolymer and 30/70 copolymer for which isothermal annealing was necessary to erase memory effects, the ESR equilibrium spectrum for the PMA4 40/60 copolymer was quickly reached and no particular thermal procedure was needed to obtain reproducible results. This feature may be associated with the non-mesogenic nature of the 40/60 copolymer. The temperature dependences of  $\tau_{||}$  for the copolymers are shown in Figure 3.

Very similar trends are apparent for both copolymers. Above  $T_g$ , two different dynamic regions, namely high temperature and intermediate temperature regions, were detected (Figure 3). The temperature dependences of  $\tau_{||}$  for both fast and slow components could individually be described by the VF law. The values of the fit parameters for the two copolymers are compared in Table 6. Homogeneous substrates are formed in both copolymers,

**Table 5.**

Fit parameters for the VF temperature dependence of cholestane spinning correlation time in the PMA4 homopolymer for the fast (F) and slow (S) sites in the high (H) and intermediate (I) temperature regions.

T region	$\tau_{  \infty}$ (s)	$T_o$ (K)	$T_b$ (K)
$T_a = 383$ K			
HT (F)	$(1.2 \pm 0.1) \cdot 10^{-11}$	$259 \pm 3$	$608 \pm 27$
IT (F)	$(1.4 \pm 0.1) \cdot 10^{-9}$	$258 \pm 8$	$164 \pm 9$
HT (S)	$(3.3 \pm 0.3) \cdot 10^{-10}$	$259 \pm 3$	$497 \pm 4$
IT (S)	$(3.6 \pm 0.3) \cdot 10^{-8}$	$259 \pm 4$	$47 \pm 2$
$T_a = 358$ K			
HT (F)	$(3.3 \pm 0.2) \cdot 10^{-12}$	$258 \pm 9$	$799 \pm 60$
IT (F)	$(3.0 \pm 0.2) \cdot 10^{-10}$	$258 \pm 7$	$258 \pm 15$
HT (S)	$(3.0 \pm 0.2) \cdot 10^{-10}$	$258 \pm 7$	$527 \pm 20$
IT (S)	$(1.6 \pm 0.1) \cdot 10^{-8}$	$258 \pm 8$	$97 \pm 7$

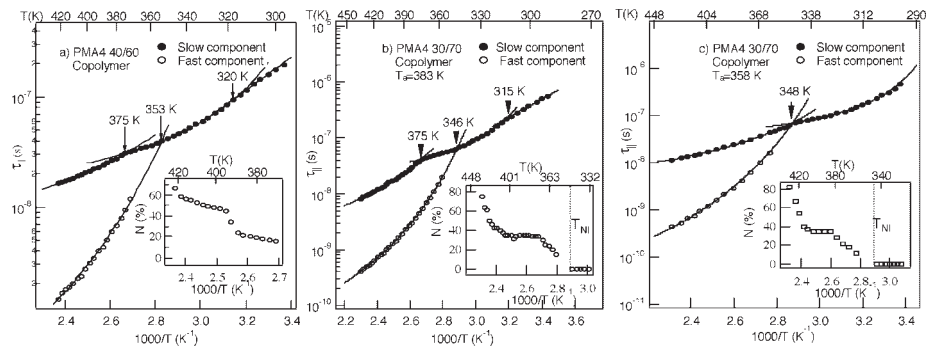


**Figure 3.** Temperature dependence of ESR correlation times in the 40/60 copolymer (a) and 30/70 copolymer for the annealing procedures at  $T_a = 383$  K (b) and  $T_a = 358$  K (c). The insets show the population ( $N$ ) of the fast component.

the fast component vanishing quickly with decreasing temperature to  $T_{NI}$  for the 30/70 copolymer. Thus, the close similarity of the dynamic behavior of the two copolymers allows for extrapolation of  $T_{NI} \approx 353$  K for the 40/60 copolymer, although the nematic-isotropic phase transition was not detected macroscopically (Figure 3a). Moreover, a crossover between the two different VF regimes occurs at a critical temperature  $T_c \approx 1.1\text{--}1.2 T_g$ , according to the mode coupling theory,<sup>[22]</sup> in both the 40/60 copolymer and the 30/70 copolymer annealed at 383 K ( $T_c \approx 375$  K). Finally, comparing the fast and slow components for the 30/70 copolymer (Figure 3) and

homopolymer (Figure 2) after they were annealed at  $T_a = 358$  K, one notes that such thermal treatment provides homogeneous substrates. This finding suggests that an optically induced bit in the copolymer could be stable well above  $T_g$  at higher temperatures than in the corresponding homopolymer.

Conclusions

The study of the dynamics of the cholestane spin probe in a series of azobenzene polymethacrylates has revealed the existence of and the crossover between different

**Table 6.** Fit parameters for the temperature dependence of cholestane spinning correlation time in the PMA4 copolymers for the fast (F) and slow (S) sites in the high (H) and intermediate (I) temperature regions.

T region	$\tau_{  } \propto$ (s)	$T_0$ (K)	$T_b$ (K)
40/60 Copolymer			
HT (F)	$(1.4 \pm 0.3) \cdot 10^{-11}$	$258 \pm 4$	$760 \pm 60$
HT (S)	$(3.2 \pm 0.3) \cdot 10^{-9}$	$258 \pm 4$	$263 \pm 25$
IT (S)	$(9.4 \pm 0.2) \cdot 10^{-9}$	$258 \pm 4$	$138 \pm 12$
30/70 Copolymer ( $T_a = 383$ K)			
HT (F)	$(4.8 \pm 0.3) \cdot 10^{-12}$	$266 \pm 4$	$778 \pm 62$
IT (F)			
HT (S)	$(4.4 \pm 0.3) \cdot 10^{-10}$	$266 \pm 5$	$493 \pm 39$
IT (S)	$(1.1 \pm 0.2) \cdot 10^{-8}$	$266 \pm 5$	$147 \pm 12$
30/70 Copolymer ( $T_a = 358$ K)			
HT (F)	$(2.9 \pm 0.2) \cdot 10^{-12}$	$266 \pm 7$	$820 \pm 70$
IT (F)			
HT (S)	$(2.0 \pm 0.1) \cdot 10^{-9}$	$266 \pm 6$	$290 \pm 20$
IT (S)	$(2.2 \pm 0.1) \cdot 10^{-8}$	$266 \pm 8$	$94 \pm 6$

dynamic regimes as function of temperature. In particular, special signatures are recognized at  $T_g$ ,  $T_{\text{conf}}$ ,  $T_{\text{NI}}$ , and  $T_c$  depending on the chemical structure of the polymer. The last crossover temperature is only detected in the copolymers according to the molecular sites available to the spin probe for reorientation.

Of special relevance appears the capability of the ESR spectroscopy to identify annealing processes effecting the best suited homogeneity on the nanoscale for optical writing. This seems to be provided by the 30/70 copolymer after annealing at a temperature slightly above  $T_{\text{NI}}$ .

- [1] R. H. El Halabieh, O. Mermut, C. J. Barrett, *Pure Appl. Chem.* **2004**, 76, 1445.
- [2] A. Natansohn, P. Rochon, *Chem. Rev.* **2002**, 102, 4139.
- [3] V. Likodimos, M. Labardi, L. Pardi, M. Allegrini, M. Giordano, A. Arena, S. Patanè, *Appl. Phys. Lett.* **2003**, 82, 3313.
- [4] L. Andreozzi, M. Faetti, G. Galli, M. Giordano, D. Palazzuoli, *Macromol. Symp.* **2004**, 218, 323.
- [5] L. Andreozzi, M. Faetti, M. Giordano, D. Palazzuoli, G. Galli, *Macromolecules* **2001**, 34, 7325.
- [6] F. D. Tsay, A. Gupta, *J. Polym. Sci., Polym. Phys. Ed.* **1987**, 25, 855.
- [7] Z. Veksli, M. Andreis, B. Rakinov, *Prog. Polym. Sci.* **2000**, 25, 948 and references therein.
- [8] P. P. Kamaev, I. I. Aliev, A. L. Iordanskii, A. M. Wasserman, *Polymer* **2001**, 42, 515.
- [9] L. Andreozzi, C. Autiero, M. Faetti, M. Giordano, F. Zulli, *J. Phys.: Condens. Matter* **2006**, 18, 6481.
- [10] M. Faetti, M. Giordano, D. Leporini, L. Pardi, *Macromolecules* **1999**, 32, 1876.
- [11] D. Xu, D. E. Budil, C. K. Ober, J. H. Freed, *J. Phys. Chem.* **1996**, 100, 15867.
- [12] L. Andreozzi, M. Giordano, M. Faetti, D. Palazzuoli, *Appl. Magn. Res.* **2002**, 22, 71.
- [13] A. S. Angeloni, D. Caretti, M. Laus, E. Chiellini, G. Galli, *J. Polym. Sci., Polym. Chem. Ed.* **1991**, 29, 1865.
- [14] Y. Tian, K. Watanabe, X. Kong, J. Abe, T. Iyoda, *Macromolecules* **2002**, 35, 3739.
- [15] L. Andreozzi, C. Autiero, M. Faetti, M. Giordano, F. Zulli, I. Szanka, G. Galli, *Mol. Cryst. Liq. Cryst.* in press.
- [16] L. Andreozzi, M. Faetti, G. Galli, M. Giordano, D. Palazzuoli, *Mol. Cryst. Liq. Cryst.* **2004**, 411, 515.
- [17] M. Giordano, P. Grigolini, D. Leporini, P. Marin, *Phys. Rev. A* **1983**, 28, 2474.
- [18] S. G. Carr, S. K. Kao, G. R. Luckhurst, C. Zannoni, *Mol. Cryst. Liq. Cryst.* **1976**, 35, 7.
- [19] L. Andreozzi, M. Giordano, D. Leporini, *Appl. Magn. Res.* **1993**, 4, 279.
- [20] L. Andreozzi, A. Di Schino, M. Giordano, D. Leporini, *Europhys. Lett.* **1997**, 38, 669.
- [21] S. Matsuoka, *J. Res. Natl Inst. Stand. Technol.* **1997**, 102, 213.
- [22] W. Goetze, L. Sjoegren, *Rep. Prog. Phys.* **1992**, 55, 55 and references therein.